Testing of the transionospheric radiochannel using data from the global GPS network

Afraimovich E. L., Karachenschev V. A.

Institute of Solar-Terrestrial Physics SD RAS,

p. o. box 4026, Irkutsk, 664033, Russia

fax: +7 3952 462557; e-mail: afra@iszf.irk.ru

Short title: GPS TESTING OF THE TRANSIONOSPHERIC RADIOCHANNEL

Abstract.

Using the international ground-based network of two-frequency receivers of the GPS navigation system provides a means of carrying out a global, continuous and fully-computerized monitoring of phase fluctuations of signals from satellite-borne radio engineering systems caused by the Earth's inhomogeneous and nonstationary ionosphere. We found that during major geomagnetic storms, the errors of determination of the range, frequency Doppler shift and angles of arrival of transionospheric radio signals exceeds the one for magnetically quiet days by one order of magnitude as a minimum. This can be the cause of performance degradation of current satellite radio engineering navigation, communication and radar systems as well as of superlong-baseline radio interferometry systems.

1. Introduction

Radio engineering satellite systems (RESS), with their ground-based and space-borne support facilities, are finding ever-widening application in various spheres of human activity. They are able to provide global coverage, accuracy, continuity, high reliability and meet a number of other requirements imposed when tackling a broad spectrum of engineering problems. However, the use of RESS also implies new (and, in some cases, more stringent) requirements dictated by the need to ensure safety and economical efficiency of the operation of ground-based and airborne facilities, as well as to solve special problems (observation, aerophotography, searching and rescue of distressed transport vehicles and people). This applies equally for performance of Global Navigation Satellite Systems (GNSS) as well as for very-long-baseline radio interferometers (VLBI) [*Thompson, R. et al.*, 1986].

Such requirements cannot be met unless the influence of destabilizing factors in the radio wave propagation channel is taken into account. As electromagnetic waves propagate through the ionosphere, they experience quite varied disturbances [*Davies*, 1969; *Kolosov et al.*, 1969; *Yakovlev*, 1985; *Goodman and Aarons*, 1990; *Yakubov*, 1997].

The key characteristic of the ionosphere that determines the variation of radio wave parameters is the integral (total) electron content (TEC) $I(t)$ or its derivatives (with respect to time and space) I'_t, I'_x and I'_y along the propagation path.

TEC variations may be arbitrarily classified as regular and irregular. Regular changes (seasonal, diurnal) - for the magnetically quiet mid-latitude ionosphere at least - are described by models providing relative accuracy of TEC prediction in the range 50...80%. Irregular changes (variations) are associated with ionospheric irregularities of a different nature, the spectrum of which has a power law character [*Gajlit*, 1983; *Gershman et al.*, 1984; *Yakubov*, 1997].

TEC variations introduce proportionate changes of the signal phase $\varphi(t, x, y) = k_1 I(t, x, y)$, which gives rise to measuring errors of the range $\sigma D = k_2 dI$, the frequency Doppler shift of the signal $\sigma f = k_3 I'_t$, and the angles of arrival of the radio wave $\sigma \alpha_x = k_4 I'_x$ and $\sigma \alpha_y = k_4 I'_y$, because the last

four quantities are proportional to the time and space derivatives of the phase. Furthermore, the maximum value of the measuring error of angular deviations can be deduced using the relation $\sigma\alpha = k_4 \sqrt{(I'_x)^2 + (I'_y)^2}$.

The coefficients $k_1 - k_4$ are inversely proportional to the signal frequency f_c or to its square [*Davies*, 1969; *Kravtsov et al.*, 1983; *Goodman and Aarons*, 1990]. A calculation uses a Cartesian topocentric coordinate system with the axis x pointing eastward E, and the axis y pointing northward N.

Investigations of phase fluctuations of transionospheric signals have been and are carried out using radio beacons on satellites with circular and geostationary orbits [*Komrakov and Skrebkova*, 1980; *Livingston et al.*, 1981; *Gajlit*, 1983]. The trouble with these measurements is that temporal and spatial resolution is low, and continuity and global coverage of observations are unavailable.

The use of the international ground-based network of two-frequency receivers of the navigation GPS system that at the beginning of 2002 consisted of no less than 1000 sites and is posting its data on the Internet, opens up new avenues for a global, continuous, fully computerized monitoring of phase fluctuations of signals and associated errors of RESS performance.

Some research results on the prediction and estimation of radio signal fluctuations and errors of RESS performance caused by them were reported in earlier work [*Afraimovich and Karachenschev*, 2002].

Results of experimental investigations of phase fluctuations of RESS signals that are discussed in this paper were derived from analyzing the data for a set consisting of 100 to 300 GPS stations covering the time interval 1998-2001, for different conditions of geomagnetic activity (the D_{st}-index from -13 to -377 nT). The number of passes of GPS satellites with a duration of no less than 2.5 hours, the data from which were used in the analysis, totaled no less than 300000, or several orders of magnitude in excess of the currently available statistic of such measurements.

Below we give an outline of the techniques used in this study and illustrate their application in the analysis of ionospheric effects. The overall sample statistic of errors σD, σf and $\sigma\alpha$ is presented for different geomagnetic conditions. To ease

comparison with other research results reported in [*Gajlit*, 1983; *Kravtsov et al.*, 1983], the errors σD, σf and $\sigma \alpha$ are calculated for the working frequency of 300 MHz.

2. General information about the database used

This study relies on the data from the global network of receiving GPS stations available on the Internet (Fig. 1). As is evident from Fig. 1, the receiving sites are relatively dense on the territory of North America and Europe, and less as dense in Asia. Fewer stations are located on the Pacific and Atlantic.

Such coverage of the terrestrial surface by GPS receivers makes it possible, already at the present time, to address the problem of a global investigation of ionospheric disturbances and their consequences with a very large spatial accumulation.

Thus, in the Western hemisphere the corresponding number of stations is as large as 500, and the number of line-of-sight (LOS) to the satellite is at least 2000...3000. This provides a number of statistically independent series at least two orders of magnitude higher than would be realized by recording VHF radio signals from first-generation geostationary satellites or low-orbit navigation satellites - TRANSIT [*Gershman et al.*, 1984].

Our analysis used the North-American sector with a large number of GPS station – range of longitudes -120° ... -60° E and of latitudes 20° ... 70° N. Table 1 presents information about number of the days, the number n of GPS arrays composed of three stations, the data from which are used, and extreme values of $D_{st_{min}}$. Total number of spectra Σ also is resulted which were used for definition of average sizes of inclinations.

For a variety of reasons, for the various events to be analyzed, we selected somewhat differing sets of receiving stations, yet the geometry of the experiment was virtually identical for all events. The coordinates of the receiving stations used in the experiment were available at the electronic address: ftp://lox.ucsd.edu/pub.processing/gamit/setup/coords.txt.

3. Analysis of the measuring errors of the range, Doppler frequency and angles of arrival of the radio wave caused by changes in the regular ionosphere

Recently a number of authors [*Wilson et al.*, 1995; *Mannucci et al.*, 1998; *Schaer et al.*, 1998; *and others*] have developed a new technology for constructing Global Ionospheric Maps (GIM) of TEC using IONEX data from the international IGS-GPS network. The GIM technology and its uses have been reported in a large number of publications [*Wilson et al.*, 1995; *Mannucci et al.*, 1998].

The standard IONEX format is described in detail in [*Schaer et al.*, 1998]. Therefore, we will not give a detailed description of the GIM technology for reasons of space but limit ourselves only to the information required for the presentation of our method. Two-hour TEC maps are easily accessible to any user, which are calculated by several research groups in the USA and Europe and are availabe on the Internet in the standard IONEX format (ftp://cddisa.gsfc.nasa.gov/pub/gps/products/ionex). It is also possible to obtain 15-min maps if necessary.

Fig. 2 is a schematic representation of a single elementary GIM cell. The cell nodes are designated as a, b, c, d. The cell size ($5°$ in longitude and $2.5°$ in latitude) is determined by the IONEX file standard. For simplifying the transformations to an approximation sufficient for our problem for latitudes not exceeding $60°$, the cell can be represented as a rectangle with the sides d_e and d_n. It is easy to overcome this limitation by complicating to a certain extent the transformations allowing for the sphericity; however, we do not present them in this report.

The linear size of the rectangular cell in latitude is independent of the latitude and is $d_e = 279$ km; the linear size in longitude depends on the latitude, and for $40°N$ it is $d_n = 436$ km.

For each time t, for the nodes a, b, c, d from the IONEX file the values of vertical TEC are known - I_a, I_b, I_c, I_d.

The determination of the range D by the phase method is based on measuring the phase difference φ between the received signal and the reference signal formed in the receiver. Such a measurement can be made at the intermediate or carrier

frequency of the signal. In this case:

$$D = c \times \frac{\varphi}{2 \pi f_c} \tag{1}$$

where c is the propagation velocity of radio waves in a free space.

Generally the quantity φ for the transionospheric propagation may be regarded as the sum of two components [*Afraimovich et al.*, 1998]:

$$\varphi = \varphi_s + \Delta\varphi \tag{2}$$

where φ_s is the main component associated with a change of the distance between the signal source and the receiver.

Analysis of the measuring errors of the range, Doppler frequency and angles of arrival of the radio wave caused by changes in the regular ionosphere investigations of global phase variations of radio signals and their influence on the operation of RESS ought to take into account the proportionate relationship between phase (phase derivative) changes of the transionospheric signal and corresponding TEC variations [*Kravtsov et al.*, 1983; *Goodman and Aarons*, 1990]:

$$\Delta\varphi = 8.44 \times 10^{-7} \times \frac{I_{a(b,c,d)}}{f_c} + \varphi_0 \tag{3}$$

where f_c is the radio wave frequency (Hz); $I_{a(b,c,d)}$ is the TEC measured at the points a, b, c, and d (10^{16} $^{el}/_{m^2}$); and φ_0 is the initial phase [*Spoelstra and Kelder*, 1984].

By way of example we now analyze the errors of measurement of the range σD, the frequency Doppler shift σf and the angle of arrival of the radio wave $\sigma\alpha$ using the IONEX data and the method that was developed at the ISTP SB RAS [*Afraimovich and Karachenschev*, 2002].

The change of the range that is introduced by the ionosphere (ionospheric error) is proportional to $\Delta\varphi$:

$$\sigma D = c \times \frac{\Delta\varphi}{2 \pi f_c} \tag{4}$$

Upon substituting (3) into (4), we can obtain the expression for determining the measuring error of the range σD introduced by the ionosphere:

$$\sigma D = \frac{c \times 8.44 \times 10^{-7} \times dI}{2 \pi f_c^2} = 4.48 \times dI \tag{5}$$

As is seen from (5), the error σD is directly proportional to the TEC variation dI and inversely proportional to the carrier frequency squared.

Using the values of the spatial derivatives of TEC I'_x and I'_y and of the derivative of TEC with respect to time I'_t makes it possible to uniquely obtain - for each instant of time - the values of errors of determination of the angle of arrival $\sigma \alpha$ and the frequency Doppler shift σf by formulas [*Kravtsov et al.*, 1983; *Goodman and Aarons*, 1990]:

$$\sigma f = \frac{1.39 \times 10^2}{f_c^2} \times \sqrt{(I'_x)^2 + (I'_y)^2} \tag{6}$$

$$\sigma \alpha = \frac{1.34 \times 10^{-7}}{f_c} \times I'_t \tag{7}$$

In the simplest case, the values of the derivatives for the selected cell of the map can be obtained using TEC increments for the four cell nodes and for two times t_1 and $t_2 = t_1 + d_t$:

$$
\begin{aligned}
dI &= (I_{a2} - I_{a1} + I_{b2} - I_{b1} + I_{c2} - I_{c1} + I_{d2} - I_{d1})/4 \\
\Delta I'_t &= (I_{a2} - I_{a1} + I_{b2} - I_{b1} + I_{c2} - I_{c1} + I_{d2} - I_{d1})/4d_t \\
\Delta I'_x &= (I_{c1} - I_{b1} + I_{d1} - I_{a1} + I_{c2} - I_{b2} + I_{d2} - I_{a2})/4d_e \\
\Delta I'_y &= (I_{a1} - I_{b1} + I_{d1} - I_{c1} + I_{a2} - I_{b2} + I_{d2} - I_{c2})/4d_n
\end{aligned} \tag{8}
$$

Where necessary, the spatial derivatives can be estimated by taking into account the TEC values in adjacent nodes of the map, and the time derivative (with a time resolution of IONEX maps no worse than 15 min) can be inferred by averaging increments for several successive time counts.

The procedures (5), (6) and (7) are performed for all cells of the selected spatial range and for the selected time interval of the day. One variant of data representation implies a full exploitation of the IONEX format with the difference that, rather than the values of TEC and the error of TEC determination [*Schaer et al.*, 1998], are entered into the corresponding cells of the map values of error σD, σf and $\sigma \alpha$.

By way of example, it is appropriate to give the results derived from analyzing the regular part of the spatial-temporal TEC variations for a relatively magnetically quiet day of July 29, 1999 (with the largest deviation of the D_{st}-index of -40 nT) and for the magnetically disturbed day of April 6, 2000 (with the largest deviation of the D_{st}-index of -293 nT).

Fig. 3 a, b, c portrays the maps of the errors σD, σf and $\sigma \alpha$ obtained on the basis of files in the IONEX format for the magnetically quiet day of July 29, 1999 in the geographic coordinate system in the range of longitudes -120° ... -60° E and latitudes 20° ... 70° N. Fig. 3 d, e, f, respectively, characterizes the values of σD, σf and $\sigma \alpha$ for the magnetically disturbed day of April 6, 2000. The figure also shows the time interval 19-21 UT, for which the analysis was carried out. Contours show the values of errors of phase measurements in units, respectively, of σD - "m" (meters), σf - "Hz" (Hertz), and $\sigma \alpha$ - "arcmin" (minutes of arc). The vertical calibrated scale shows the maximum and minimum values of the corresponding errors.

The above maps are a pictorial rendition of the behavior dynamics of the errors σD, σf and $\sigma \alpha$ in the spatial and temporal ranges selected. Noteworthy is a considerable difference of the maps for the magnetically quiet and disturbed days. As is evident from Fig. 3, gradients of spatial distribution of the errors during disturbances increase more than an order of magnitude when compared to the quiet period, which would lead to a degradation of RESS performance.

4. Analysis of the irregular errors σD, σf and $\sigma \alpha$

Our analysis of the irregular component of the errors was based on using raw data in the form of series of TEC values for selected receiving sites as well as values of elevations $\Theta_s(t)$ and azimuths $\alpha_s(t)$ to visible satellites that were calculated using a specially developed program, CONVTEC, to convert RINEX-files (standard files for the GPS system) available from the Internet [*Afraimovich et al.*, 1998].

Fig. 4 presents the geometry of transionospheric radio sounding. The axes z, y, x are pointing, respectively, to the zenith, the north N, and to the east E; P is the point of intersection of the LOS to the satellite (the line connecting the

satellite to the radio signal receiver) with the ionospheric F_2 region peak; S is the subionospheric point (projection of the point P onto the terrestrial surface).

The GPS technology provides the means of estimating TEC variations on the basis of phase measurements of TEC I in each of the spaced two-frequency GPS receivers using the formula [*Hofmann-Wellenhof et al.*, 1992]:

$$I_0 = \frac{1}{40.308} \frac{f_1^2 f_2^2}{f_1^2 - f_2^2} [(L_1 \lambda_1 - L_2 \lambda_2) + \text{const} + nL], \tag{9}$$

where $L_1 \lambda_1$ and $L_2 \lambda_2$ are phase path increments of the radio signal, caused by the phase delay in the ionosphere (m); L_1 and L_2 are the number of full phase rotations, and λ_1 and λ_2 are the wavelengths (m) for the frequencies f_1 and f_2, respectively; *const* is some unknown initial phase path (m); and nL is the error in determination of the phase path (m).

Series of the values of elevations $\Theta_s(t)$ and azimuths $\alpha_s(t)$ of the beam to the satellite were used to determine the coordinates of subionospheric points, and to convert the "oblique" TEC $I_0(t)$ to the corresponding value of the "vertical" TEC $I(t)$ by employing the technique reported by [*Klobuchar*, 1986]:

$$I = I_0 \times \cos \left[arcsin \left(\frac{R_z}{R_z + h_{max}} cos\Theta_s \right) \right], \tag{10}$$

where R_z is the Earth's radius, and h_{max}=300 km is the height of the F_2-layer maximum.

All results in this study were obtained for elevations $\Theta_s(t)$ larger than 30°.

To analyze the errors σD, σf and $\sigma \alpha$ that are cased by the irregular component of TEC variation, we make use of the relations for the respective regular errors (5), (6) and (7). The difference in the analysis of irregular errors implies a different (compared with the IONEX technique) method of determining the values of TEC and its derivatives [*Afraimovich and Karachenschev*, 2002].

The phase differences $\Delta \varphi_{x,y}$ along the axes x and y are proportional to the values of the horizontal components of TEC gradient $G_E = I'_x$ and $G_E = I'_y$.

To calculate the components of the TEC gradient I'_x and I'_y are used linear transformations of the differences of the values of the filtered TEC $(I_B - I_A)$ and $(I_B - I_C)$ at the receiving points A, B and C:

$$I'_x = \frac{y_A(I_B - I_C) - y_C(I_B - I_A)}{x_A y_C - x_C y_A}; \quad I'_y = \frac{x_C(I_B - I_A) - x_A(I_B - I_C)}{x_A y_C - x_C y_A} \qquad (11)$$

where x_A, y_A, x_C, y_C are the coordinates of the sites A and C in the topocentric coordinate system. When deriving (11) we took into account that $x_B = y_B = 0$, since site B is the center of topocentric coordinate system.

The time derivative of TEC I'_t is determined by differentiating $I(t)$ at the point B.

The procedures of (5), (6) and (7) are performed for all groups of three GPS stations of the selected spatial range and for satellites visible from these stations, as well as for the selected time interval of the day.

Fig. 5 presents the results derived from analyzing the irregular component of the errors σD, σf and $\sigma \alpha$ in the form of fluctuation spectra of the range, Doppler frequency and angles of arrival of radio waves.

With the purpose of improving the statistical reliability of the data, we used the spatial averaging technique for spectra within the framework of a novel technology [*Afraimovich et al.*, 2001]. The method implies using an appropriate processing of TEC variations that are determined from the GPS data, simultaneously for the entire set of GPS satellites (as many as 5–10 satellites) "visible" during a given time interval, at all stations of the global GPS network used in the analysis.

Individual spectra of the errors σD, σf and $\sigma \alpha$ were obtained by processing continuous series of $I(t)$ measurements of a duration no shorter than 2.5 hours. To eliminate errors caused by the regular ionosphere, as well as trends introduced the motion of satellites, we used the procedure of removing the linear trend by preliminarily smoothing the initial series with the selected time window of a duration of about 60 min.

Fig. 5 shows the overall character of the TEC variations $dI(t)$ that were filtered from TEC series obtained from measurements of the phase difference between two coherently coupled signals from the GPS system [*Hofmann-Wellenhof*, 1992] for the magnetically quiet day of July 29, 1999 (panel a, at the left) and a major magnetic storm of July 15, 2000 (panel e, at the right). Furthermore, the panels show the station names and locations, as well as GPS satellite numbers (PRN).

As is evident from the figure, the intensity $dI(t)$ during the disturbance even at such low latitudes is increased an order of magnitude as a minimum. This is reflected on logarithmic amplitude spectra $lgS(F)$ of TEC fluctuations and their derivatives (left-hand scale in the figures) and of the fluctuations of σD, σf and $\sigma \alpha$, converted to the working frequency of 300 MHz (right-hand scale) which are represented on a logarithmic scale (panels b, c, d, f, g, h).

The logarithmic amplitude spectrum $lgS(F)$ obtained by using a standard FFT procedure. Incoherent summation of the partial mplitude spectra $lgS(F)_i$ of different LOS was performed by the formula:

$$lg\langle S(F)\rangle = lg\left[\frac{\sum\limits_{i=1}^{n} S(F)_i}{n}\right] \tag{12}$$

where i is the number of LOS; $i = 1, 2, ... \ n$.

As a consequence of the statistical independence of partial spectra, the signal/noise ratio, when the average spectrum is calculated, increases due to incoherent accumulation at least by a factor of $\sqrt{n}$, where n is the number of LOS.

Fluctuation spectra from the magnetically quiet day of July 29, 1999 are shown by the thin line in panels f, g, h (Fig. 5) for comparison with the spectra from the disturbed day. The range of fluctuation periods is shown in bold type along the abscissa axis in panels d and h. Panels b and f show also the number n of GPS arrays composed of three stations, the data from which are used to estimate the spatial derivatives of TEC [*Afraimovich et al.*, 2001].

Spectra of phase fluctuations have a power law character with the values of the slopes ν, shown in panels b, c, d, f, g, h. The slope of spectrum is determined by the slope of the fitted straight line (thin black line in panel b of Fig. 5). These results are in reasonably good agreement with data reported in [*Komrakov and Skrebkova*, 1980; *Livingston et al.*, 1981; *Gajlit et al.*, 1983; *Kravtsov et al.*, 1983; *Gershman et al.*, 1984; *Yakubov*, 1997].

5. Distribution of slopes and scales of spectra of the errors

In the preceding section we obtained the fluctuation spectra of the errors σD, σf and $\sigma \alpha$ corresponding to different ionospheric conditions. It was shown that the spectra have a power law character, with definite indices of the slope ν (Fig. 5). However, the individual spectra that were obtained do not give a full insight into the global picture of fluctuations of the errors. To obtain a generalized estimate we carried out an analysis of the spectra of errors obtained by processing the data covering more than 30 days (over 600 spectra).

In our experiment the range of fluctuation periods of spectra varies from 2 min to 2 hours. Experimental spectra of the errors σD, σf and $\sigma \alpha$ have a complicated form (Fig. 5). There are spectral density maxima and minima. Generally, however, the spectral density $S(F)$ decreases with the increasing fluctuation frequency. For each individual spectrum, calculated on a logarithmic scale, we determined the fitted straight line.

The result of a generalized estimation is represented by the plots in Fig. 6. The plots show the distributions of the slopes $P_{\sigma D}(\nu)$, $P_{\sigma f}(\nu)$, $P_{\sigma \alpha}(\nu)$ of power law spectra of the errors σD, σf and $\sigma \alpha$, respectively. The interval $\Delta \nu$ of the slopes of the spectra σD is $\Delta_{\sigma D} = -1.45...2.45$, with the mean value of $<\Delta_{\sigma D}> = -1.95$. In view of the relationship between the spectrum $\sigma D \sim \varphi(t)$ and the spectra σf and $\sigma \alpha$ that are proportional to the derivative of $\varphi(t, x, y)$ ($\sigma f \sim \varphi'(t)$ and $\sigma \alpha \sim \varphi'(x, y)$), for the slopes of the spectra σf and $\sigma \alpha$ these values are, respectively, $\Delta_{\sigma f} = -0.40...1.60$, $<\Delta_{\sigma f}> = -0.99$ and $\Delta_{\sigma \alpha} = -0.40...2.00$, $<\Delta_{\sigma \alpha}> = -1.8$. Our results are in good agreement with findings reported by a number of authors [*Gajlit et al.*, 1983].

The fitted straight line (the slant thin black line in panel *b*, Fig. 5) for the logarithmic scale of errors in range may be described by the expression (13):

$$Y = a \times X + b \tag{13}$$

here a characterizes the slope of the straight line, and b is the scale coefficient characterizing the rise of the straight line with respect to the abscissa axis, that is, the value of Y_0 when $X_0 = 0$.

The value of $lgS^{\sigma D}(F)$ can be determined from a single (previously determined) set of values of $lg(F)$, $\nu_{\sigma D}$ and $b_{\sigma D}$ on the basis of the expression:

$$lgS^{\sigma D}(F) = \nu_{\sigma D} \times lg(F) + b_{\sigma D} \qquad (14)$$

Using (14) and the resulting value of $b_{\sigma D}$ and $\nu_{\sigma D}$ we can determine the value of any spectral component of $lgS^{\sigma D}(F)$ and determine its contribution to the total error. Proceeding in a similar way, we can describe the spectral characteristics of σf and $\sigma \alpha$.

Panels a, b, c in Fig. 7 presents the distributions of the values of the scales of power law spectra of the errors $b_{\sigma D}$, $b_{\sigma f}$ and $b_{\sigma \alpha}$ obtained for the entire set of data (over 600 spectra).

Let us estimate the amplitude $lgS_0^{\sigma D}$ of the 32-minute harmonic F_0 of the spectrum of the errors σD (Fig. 5) by making use of the values of $<\nu_{\sigma D}> = -1.96$ (Fig. 6) and $< b_{\sigma D} > = -6.59$ (Fig. 7). Upon substituting the corresponding values into (14), we obtain $lgS_0^{\sigma D}(F_0) = -0.153$, which corresponds to $\sigma D = 0.70$ [m].

6. Conclusion

Main results of this study are as follows:

1. In this paper we have suggested a new technique for estimating the errors of RESS performance, based on using phase measurements from two-frequency receivers of the satellite navigation GPS system.

2. Fluctuation spectra of the errors are generally quite well approximated by the power function. Mean values of the slopes of spectra, obtained from the experiment, are in good agreement with data reported by other authors.

3. The errors σD, σf and $\sigma \alpha$ are conveniently estimates with a sufficient accuracy for practical purposes by using mean statistical data for indices of slopes of spectra ν and scale coefficients b.

4. Our results can be equally assigned to the estimation of the Russian GNSS – GLONASS performance quality.

References

Afraimovich, E. L., Palamartchouk, K. S. and Perevalova, N. P., GPS radio interferometry of travelling ionospheric disturbances. *J. Atmos. and Solar-Terr. Physics.*, V. 60, N. 12, pp. 1205–1223, 1998.

Afraimovich, E. L., Kosogorov, E. A., Lesyuta, O. S., Yakovets, A. F., Ushakov, I. I., Geomagnetic control of the spectrum of traveling ionospheric disturbances based on data from a global GPS network. *Ann. Geophys.*, V. 19, N. 7, pp. 723–731, 2001.

Afraimovich, E. L., Karachenschev, V. A., Range, Doppler frequency and radio wave angle-of-arrival measurement errors for satellite-based radio engineering systems caused by the Earth's ionosphere (as deduced using data from the global GPS network), *Proceedings of VIII International Symposium on radar, navigation and communication*, Voronezh, V. 2, pp. 1405–1416, 2002.

Davies, K., Ionospheric Radio Waves. *Blaisdell, Waltham, Mass.*, 1969.

Gajlit, T. A., Gusev, V. D., Erukhimov, L. M., Shpiro, P. I., Spectrum of the phase fluctuations at the ionosphere sounding, *Izv. Vuzov. Radiofizika*, V. 26, N. 7, pp. 795–801, 1983.

Gershman, B. N., Erukhimov, L. M. and Yashin, Yu. Ya. Wave Phenomena in the Ionosphere and Space Plasma. *Moscow: Nauka*, 1984, p. 392.

Goodman, Dj. M., Aarons, J., Ionospheric Effects on Modern Electronic System, *Proceedings of the IEEE*, V. 78, N. 3, pp. 512–528, 1990.

Hofmann-Wellenhof, B., Lichtenegger, H. and Collins, J., Global Positioning System: Theory and Practice. *Springer-Verlag, New York*, 1992, p. 327.

Klobuchar, J. A., Ionospheric time-delay algorithm for single-frequency GPS users, *IEEE Transactions of Aerospace and Electronic System, AES*, V. 23, N. 3, pp. 325–331, 1986.

Kolosov, M. A., Armand, N. A. and Yakovlev, O. I. The Propagation of Radio Waves in Space Communication. *Moscow: Svyaz*, 1969, p. 155.

Komrakov, G. P., Skrebkova, L. A., Study of parameters of ionospheric irregularities by the "Interkosmos-Kopernik 500" satellite, *Ionosfernie issledovaniya, Moscow: Sovetskoe radio*, V. 30, pp. 49–52, 1980.

Kravtsov, A. Yu., Feizulin, Z. I. and Vinogradov, A. G. The Propagation of Radio Waves Through the Earth's Ionosphere. *Moscow: Radio i svyaz*, 1983, p. 224.

Livingston, R. C., Rino, C. L., McClure, J. P., Hanson, W. B., Spectral characteristics of medium-scale equatorial F region irregularities, *J. Geophys. Res.*, V. 86, pp. 2421–2428, 1981.

Mannucci, A. J., Wilson, B. D., Yuan, D. N., Ho, C. M., Lindqwister, U. J. and Runge, T. F., A global mapping technique for GPS-drived ionospheric TEC measurements. *Radio Science*, V. 33, pp. 565–582, 1998.

Schaer, S., Gurtner, W. and Feltens, J., IONEX: The IONosphere Map EXchange Format Version 1. *Proceeding of the IGS AC Workshop, Darmstadt, Germany, February 9-11; Editor J.W.Dow*, pp. 233–247, 1998.

Spoelstra, T. A., Kelder, H., Effects produced by the ionosphere on radio interferometry. *Radio Science*, V. 19, pp. 779–788, 1984.

Thompson, R., Moran, J. and Swenson, Dj. Interferometry and Synthesis in Radio Astronomy. *John Wiley and Sons, Inc.*, 1986.

Wilson, B. D., Mannucci, A. J. and Edwards, C. D., Subdaily northern hemisphere maps using the IGS GPS network. *Radio Science*, V. 30, pp. 639–648, 1995.

Yakovlev, O. I. The Propagation of Radio Waves in Space. *Moscow: Nauka*, 1985, p. 214.

Yakubov, V. P. Doppler Very-Long-Baseline Interferometry. *Tomsk: Vodolei*, 1997, p. 246.

E. L. Afraimovich, V. A. Karachenschev, Institute of Solar-Terrestrial Physics SD RAS, p. o. box 4026, Irkutsk, 664033, Russia, fax: +7 3952 462557; e-mail: afra@iszf.irk.ru

Figure 1. The map showing the locations of the receiving stations of the global GPS system. The number of receiving sites totals no less than 1000 as of the beginning of 2002.

Figure 2. Geometry of an elementary GIM cell. Nodes of the cell are denoted a, b, c, and d. The cell size is determined by the values of $d_n = 279$ km and of d_e dependent on the cell's location latitude.

Figure 3. Maps of global distribution of measurement errors of the range σD, frequency Doppler shift σf, and of angles of arrival of radio waves $\sigma \alpha$ (left - for a magnetically quiet day, right - for a magnetically disturbed day). The errors can be evaluated from the graduated scale, shown in the figure at the right.
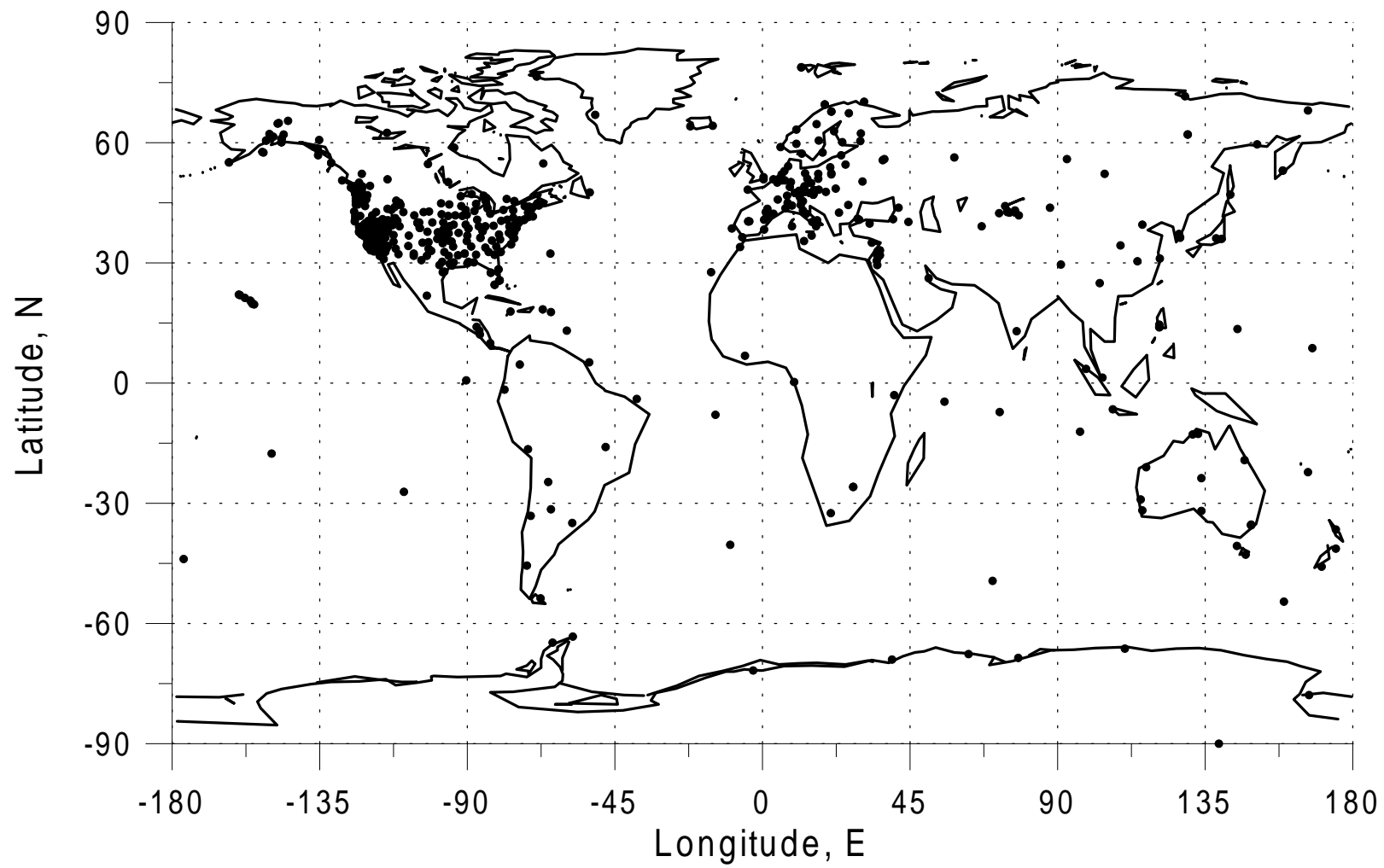
Figure 4. Schematic representation of the transionospheric sounding geometry. The axes z, y and x are directed, respectively, zenithward, northward (N) and eastward (E). P – point of intersection of Line-of-Sight (LOS) to the satellite with a horizontal plane at the height of the maximum of the ionospheric F_2 – region h_{max}; S – subionospheric point; and Θ_s, α_s – azimuth and elevation of the direction $\mathbf{r}$ along LOS to the satellite.
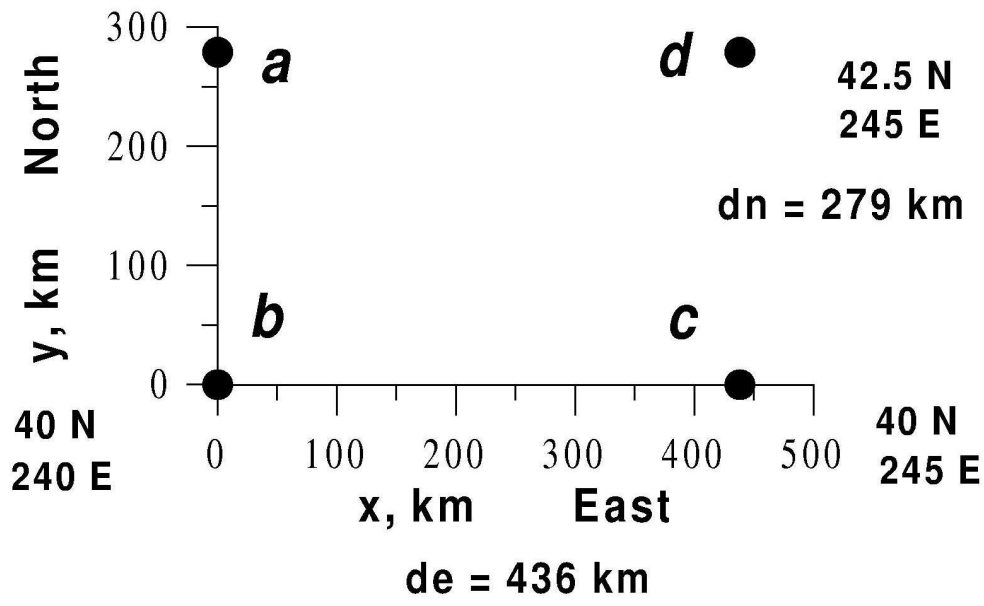
Figure 5. TEC variations $dI(t)$ for the magnetically quiet day of July 29, 1999 (left, panel a) and a major magnetic storm of July 15, 2000 (right, panel e). These panels also show the names and coordinates of the $COSA$ and $BLYT$ stations and GPS satellite numbers (PRN). Panels b,c, d, f, g, h on a logarithmic scale present the amplitude spectra $S(F)$ of TEC fluctuations and derivatives (left scale in the panels), and the fluctuation spectra of σD, σf and $\sigma \alpha$ converted to the working frequency of 300 MHz (right panel). For comparison, spectra from the magnetically quiet day of July 29, 1999 are shown in panels f, g, h by the thin line. The range of fluctuation periods is shown in bold type along the abscissa axis of panels d and h. Panels b, e show the number n of GPS arrays. The power law character of the spectra is determined by the values of slopes ν. The thin black slant line in panel b is a fitted straight line of the power law spectrum.

Figure 6. Probability distributions $P_{\sigma D}(\nu)$, $P_{\sigma f}(\nu)$ and $P_{\sigma \alpha}(\nu)$ of the slopes $\nu_{\sigma D}$, $\nu_{\sigma f}$ and $\nu_{\sigma \alpha}$ of the power law spectra of the errors σD, σf and $\sigma \alpha$. Mean values of the slopes ν, and also total numbers of the values of the slopes of the corresponding spectra use in the analysis are shown in all panels.

Figure 7. Probability distributions $P_b(\sigma D)$, $P_b(\sigma f)$ and $P_b(\sigma\alpha)$ of the scales $lg\ b_{\sigma D}$, $lg\ b_{\sigma f}$ and $lg\ b_{\sigma\alpha}$ of the power law spectra of the errors. Mean values of the slopes $<lg\ b_{\sigma D}>$ ($lg\ b_{\sigma f}>,<lg\ b_{\sigma\alpha}>$) (on a logarithmic scale), standard deviations, and also total numbers of the values of the scales of the corresponding spectra used in the analysis are shown in all panels.
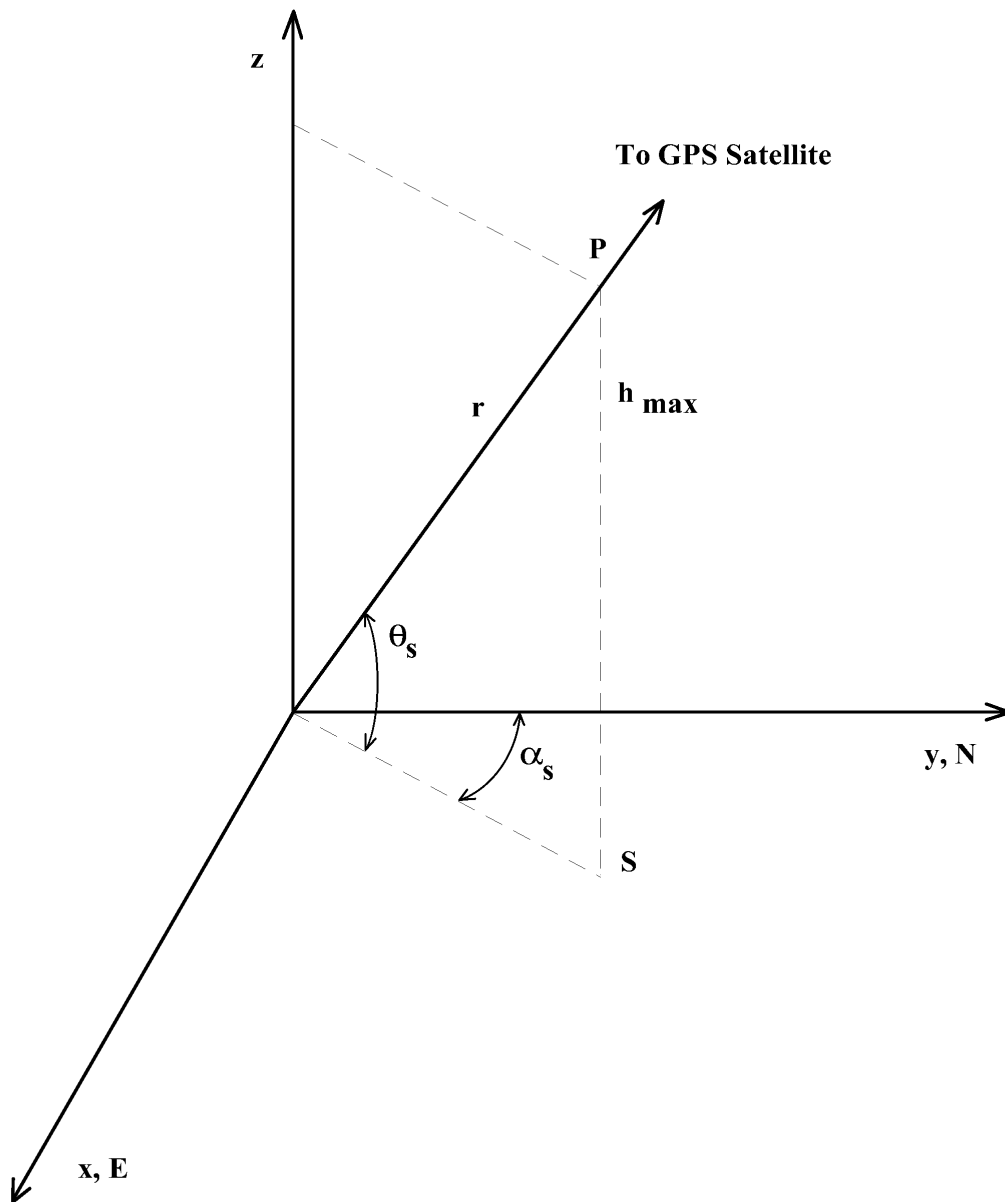
GPS global network

300

North

a

d ●

42.5 N
245 E

y, km

200

dn = 279 km

100

b

c

0

40 N
240 E

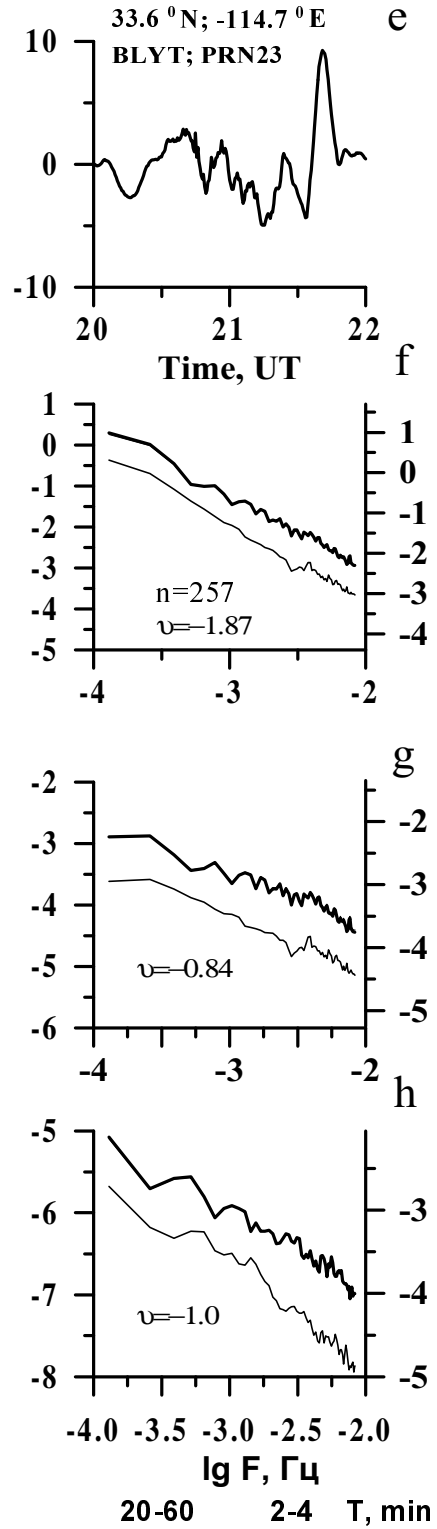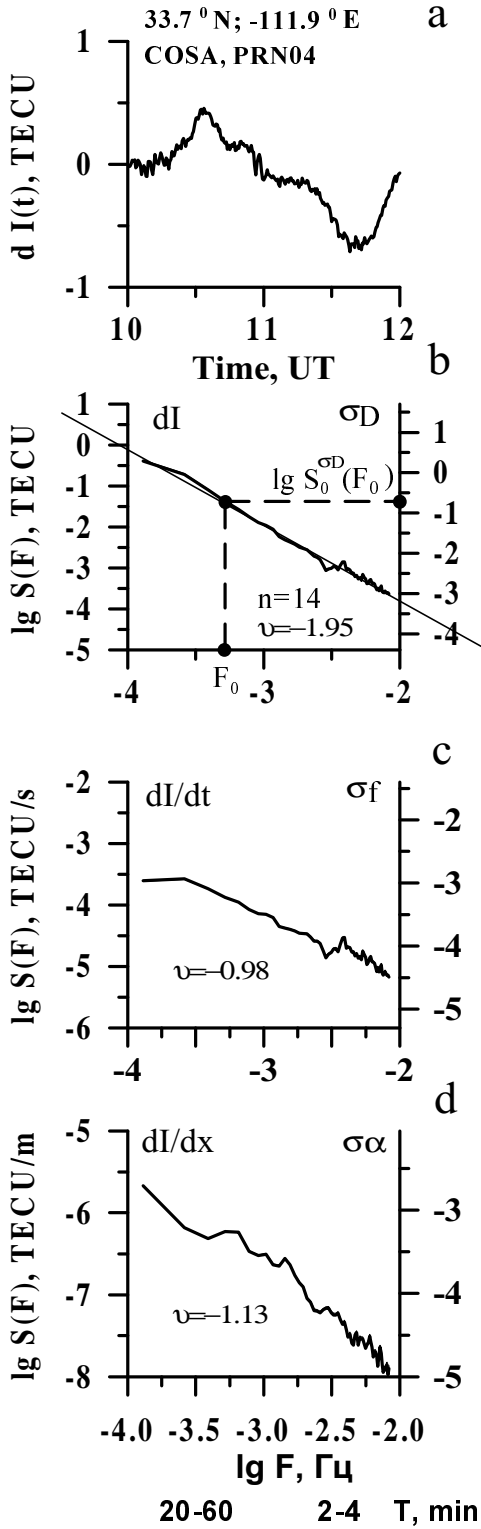0   100   200   300   400   500

x, km   East

40 N
245 E

de = 436 km

This figure "fig3TEST.jpg" is available in "jpg" format from:

http://arXiv.org/ps/physics/0210048v2

z

To GPS Satellite

P

h_{max}

r

θ_s

α_s

y, N

S

x, E

July 29, 1999

July 15, 2000

Distributions of the slopes of power law spectra of the errors

$\mathbf{P_{\sigma D}}(|\upsilon|)$

a

$<|\upsilon_{\sigma D}|> = 1,96$

$\sum\limits_{\upsilon_{\sigma D}} > 600$

$|\upsilon_{\sigma D}|$

$\mathbf{P_{\sigma f}}(|\upsilon|)$

b

$<|\upsilon_{\sigma f}|> = 0,99$

$\sum\limits_{\upsilon_{\sigma f}} > 600$

$|\upsilon_{\sigma f}|$

$\mathbf{P_{\sigma \alpha}}(|\upsilon|)$

c

$<|\upsilon_{\sigma \alpha}|> = 1,08$

$\sum\limits_{\upsilon_{\sigma \alpha}} > 600$

$|\upsilon_{\sigma \alpha}|$
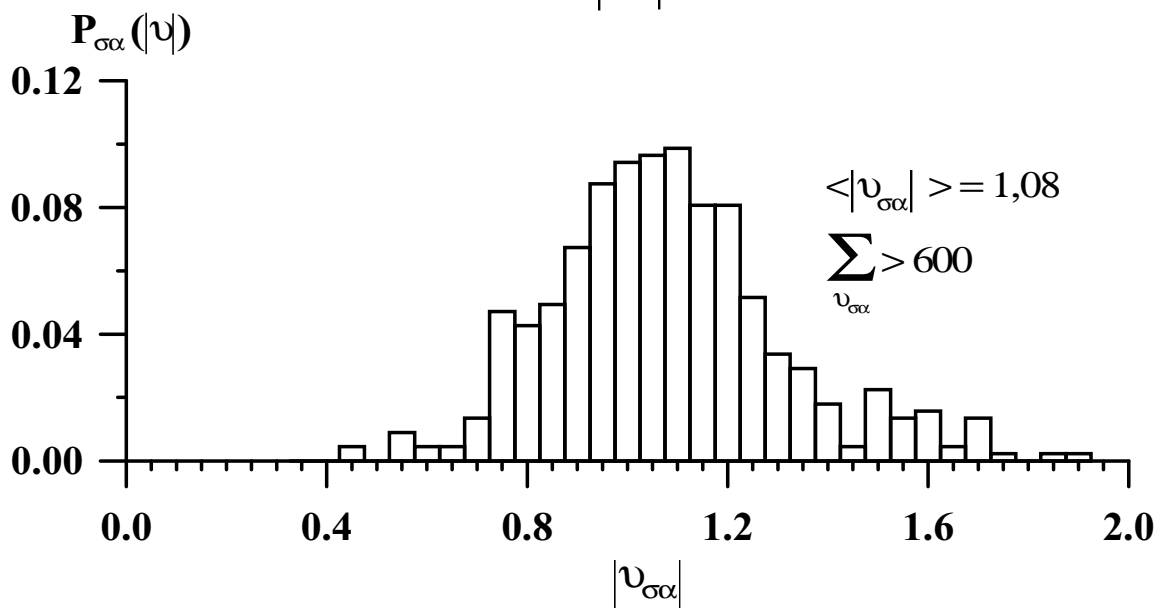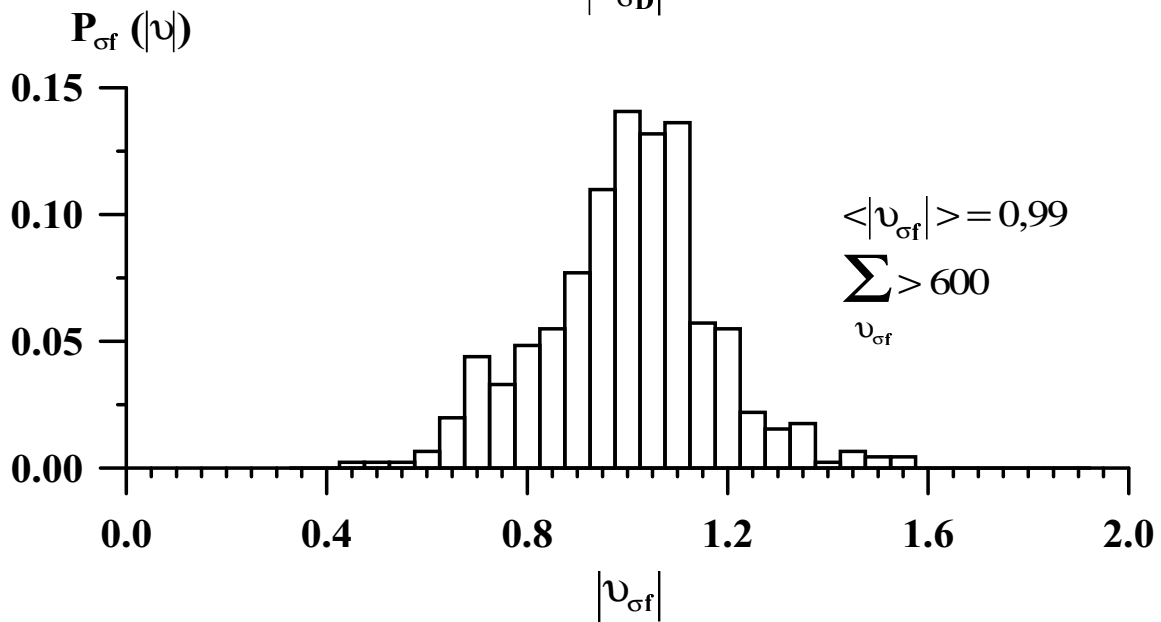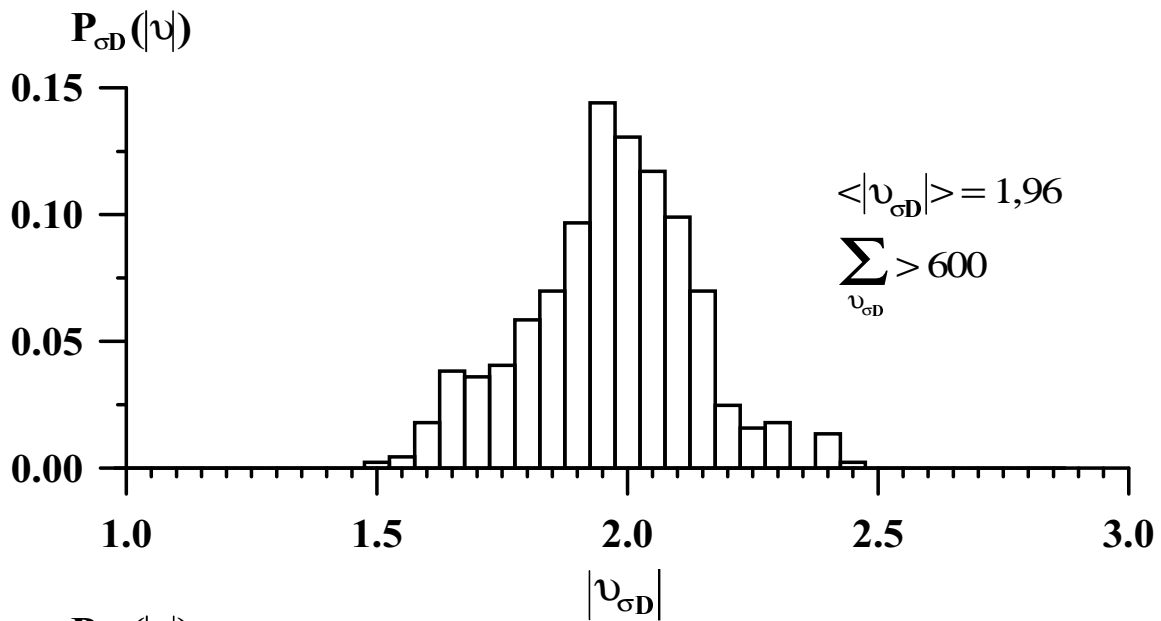
Distributions of the scales of the power law spectra of the errors

$P_b(\sigma D)$

a

$< \lg b_{\sigma D} > = -6.59$

RMS = 0.85

$\sum\limits_{b_{\sigma D}} > 600$

$\lg b_{\sigma D}$

$P_b(\sigma f)$

b

$< \lg b_{\sigma f} > = -7.15$

RMS = 1.07

$\sum\limits_{b_{\sigma f}} > 600$

$\lg b_{\sigma f}$

$P_b(\sigma\alpha)$

c

$< \lg b_{\sigma\alpha} > = -5.33$

RMS = 2.06

$\sum\limits_{b_{\sigma\alpha}} > 600$

$\lg b_{\sigma\alpha}$